available at www.sciencedirect.com

ScienceDirect

journal homepage: www.elsevier.com/locate/chnjc

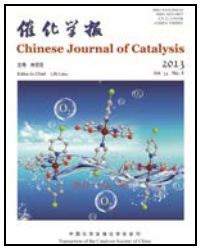

Article

Chemical and photocatalytic water oxidation by mononuclear Ru catalysts

Yi Jiang [a], Fei Li [a,*], Fang Huang [a], Biaobiao Zhang [a], Licheng Sun [a,b,#]

[a] *State Key Laboratory of Fine Chemicals, Faculty of Chemical, Environmental and Biological Science and Technology, Dalian University of Technology, Dalian 116024, Liaoning, China*

[b] *Department of Chemistry, School of Chemical Science and Engineering, KTH Royal Institute of Technology, Stockholm 10044, Sweden*

ARTICLE INFO

Article history:
Received 22 March 2013
Accepted 10 April 2013
Published 20 August 2013

Keywords:
Water splitting
Water oxidation
Ruthenium complex
Electron-withdrawing effect
Photocatalysis

ABSTRACT

Four mononuclear Ru complexes with different substituents on the *para* position of the pyridine ligand of Ru(bda)(pic)$_2$ (H_2bda = 2,2'-bipyridine-6,6'-dicarboxylic acid; pic = picoline) were synthesized and characterized by ^{1}H nuclear magnetic resonance or X-ray crystallography. The electrochemical properties of this series of compounds in acidic and neutral conditions were studied by cyclic voltammetry. Their catalytic activity towards water oxidation was investigated using a chemical oxidant ($[Ce(NH_4)_2(NO_3)_6]$ (Ce^{IV}) in acidic solution, or driven by visible light in a three-component system containing a photosensitizer ($[Ru(bpy)_3]^{2+}$) and an electron acceptor ($S_2O_8^{2-}$). For the chemical water oxidation, complex **1** was found to be the most effective, exhibiting a turnover number (TON) of up to 4000. The pyridine substituent at the 4-position in **1** may be protonated giving an intensive electron-withdrawing effect. Complex **2** bears the most electron-withdrawing trifluoromethyl group under neutral conditions and showed the highest photocatalytic activity with a TON of 270 over 2 h. It was concluded that the more electron-withdrawing substituents led to higher activity towards oxygen evolution for this type of Ru catalysts in the oxidation of water.

1. Introduction

In recent decades, much effort has been made to convert solar energy into fuels, an important step for a sustainable society in the future. Among many schemes to utilize solar energy, artificial photosynthesis to split water represents a promising method to produce H_2 from water as a clean and renewable energy store. This occurs as two half-reactions: the reduction of protons to dihydrogen and the oxidation of water to dioxygen [1–3]. Up to now, the latter half-reaction has been considered the bottleneck in the total water splitting process due to limited knowledge of the oxidation mechanism and more importantly, a lack of suitable water oxidation catalysts (WOCs).

Molecular water oxidation catalysts, with much improved efficiencies based on different transition metals, such as Mn [4,5], Ir [6–10], Co [11–14], Fe [15,16], and Ru have been reported in recent years. Among these catalysts, a number of Ru catalysts have been demonstrated to be effective in the oxidation of water [17]. In 1982, Gersten and coworkers [18] reported the first molecular dinuclear Ru compound

* Corresponding author. Tel: +86-411-84986247; Fax: +86-411-84986245; E-mail: lifei@dlut.edu.cn
# Corresponding author. Tel/Fax: +46-8-7912333; E-mail: lichengs@kth.se

This work was supported by the National Basic Research Program of China (973 Program, 2009CB220009), the National Natural Science Foundation of China (21106015, 21120102036, and 20923006), the Research Fund for the Doctoral Program of Higher Education of China (20110041120005), and the Swedish Energy Agency and K&A Wallenberg Foundation.
DOI: 10.1016/S1872-2067(12)60600-7 | http://www.sciencedirect.com/science/journal/18722067 | Chin. J. Catal., Vol. 34, No. 8, August 2013

cis,cis-$[(bpy)_2(H_2O)Ru(\mu\text{-}O)Ru(H_2O)(bpy)_2]^{4+}$ (the "blue dimer"), which was found to oxidize H_2O to O_2 with a turnover number (TON) of 13 using excess $[Ce(NH_4)_2(NO_3)_6]$ (Ce^{IV}). Inspired by the blue dimer, it was initially assumed that multiple metal centers were necessary to accomplish the water oxidation reaction. Since then, a variety of multinuclear Ru complexes have been found to be active towards water oxidation [19,20]. In 2005, Zong and Thummel [21] obtained a series of ruthenium dimers bearing a μ-Cl bridge between the two meal centers, with a TON of 3200. Recently, we reported a robust and efficient catalyst possessing a rigid ligand 1,4-bis(6′-COOH-pyrid-2′-yl)phthalazine, which exhibited a TON of more than 10000 in the presence of Ce^{IV} at pH 1.0 [22]. More recently, we have prepared a series of ruthenium dimers by linking two Ru monomer units with flexible linkers, which exhibited significant enhancement (more than an order of magnitude) in both TON and turnover frequency (TOF) with respect to their parent monomer complexes in Ce^{IV}-driven water oxidation [23]. Nevertheless, the DFT calculations of μ-O ruthenium catalysts performed by Yang and Baik [24] revealed the possibility of the key O–O bond-forming step occurring at a single catalytic site, leading to the design of mononuclear Ru complexes as potential WOCs. Two families of single-site polypyridyl mononuclear Ru complexes ($[Ru(tpy)L_2(H_2O)]^{n+}$ and $[Ru(mebimpy)L_2(H_2O)]^{n+}$, tpy = 2,2′:6′,2″-terpyridine, mebimpy = (2,6-bis(1-methylbenzimidazol-2-yl)pyridine, L = diimine ligands) have been reported by Concepcion and coworkers [25]. Our group reported a mononuclear catalyst $Ru^{II}(bda)(pic)_2$ (H_2bda = 2,2'-bipyridine-6,6'-dicarboxylic acid, pic = 4-picoline, complex **A**) bearing a negatively charged ligand, which may stabilize the high-valent ruthenium-oxo intermediate during the catalytic cycle. This complex was found to be not only a robust catalyst in Ce^{IV}-driven water oxidation but also an efficient photocatalytic water oxidation catalyst in a three-component system consisting of catalyst, photosensitizer and sacrificial electron acceptor [26–28]. We have also demonstrated that alteration of the axial ligands leads to a significant change in the kinetics of the water oxidation [29–31]. By replacing the axial picoline ligand of $Ru(bda)(pic)_2$ with isoquinoline, a high oxygen-evolving rate (300 s^{-1}) approaching that of the oxygen-evolving complex of photosystem II was acquired [29].

To understand the relationship between the structure and the water oxidation activity of the WOCs, we decided to explore the effect of the ligands on the activity of $Ru^{II}(bda)(pic)_2$ by introducing different functional groups, from electron-donating to electron-withdrawing, on the *para* position of the axial pyridine ligand. The electrochemical properties as well as the water oxidation activity of these analogues were systematically investigated.

2. Experimental

2.1. Synthesis of the mononuclear Ru complexes

Complex **1**–**4** and complex **A** were prepared by a two-step synthetic procedure as previously reported (Scheme 1) [32]. All reactions were carried out under N_2 using standard Schlenk techniques. Solvents were dried and distilled prior to use according to standard methods. $Ru(DMSO)_4Cl_2$ was prepared according to literature methods [33]. A solution of 4-chloropyridine hydrochloride was neutralized by NaOH, then extracted by CH_2Cl_2 before the solvent was removed to afford 4-chloropyridine as yellow oil. All other chemicals were commercially available and used as received.

2.1.1. Synthesis of Ru(bda)(4-Py-pic)$_2$ (complex **1**)

A mixture of 2,2′-bipyridine-6,6′-dicarboxylic acid (244 mg, 1.0 mmol), $Ru(DMSO)_4Cl_2$ (484 mg, 1.0 mmol), and Et_3N (0.8 ml) in methanol (10 ml) was degassed with N_2 and refluxed for 4 h. The solution changed from bright yellow to dark before the appearance of a brown precipitate. After cooling to room temperature, the precipitate was filtered and washed with methanol (10 ml × 3) and ether (10 ml × 3) to get a reddish-brown powder. The powder was mixed with an excess of 4,4′-bipyridine in methanol (20 ml) and heated to reflux for 2 h. The solvent was removed and the resulted residue was re-dissolved in dichloromethane, washed with water to remove triethylamine hydrochloride, and dried over $MgSO_4$ under N_2. After purification by column chromatography on silica gel with dichloromethane-methanol (20:1 to 1:1, *V*:*V*) as eluent, complex **1** was obtained as a dark red solid. Yield: 229 mg (35%). ^1H NMR (400 MHz, DMSO-d_6): δ 8.75 (d, J = 7.6 Hz, 2H), 8.66 (d, J = 4.4 Hz, 4H), 7.91–7.95 (m, 8H), 7.70 (dd, J = 4.4 Hz, 8H).

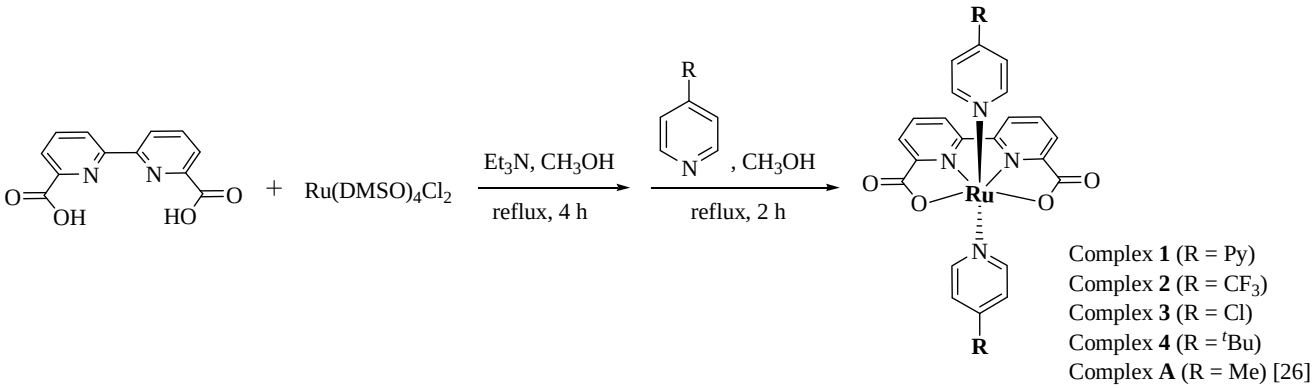

Scheme 1. Synthetic route for complexes **1**–**4**.

ESI-MS: *m/z* = 656.8 $[M + H]^+$ (calcd: 657.1), 679.0 $[M + Na]^+$ (calcd: 679.1).

*2.1.2. Synthesis of Ru(bda)(4-CF_3-pic)$_2$ (complex **2**)*

A similar procedure for the preparation of complex **1** was adopted using 4-(trifluoromethyl)pyridine (0.5 ml) as the axial ligand. Complex **2** was obtained as a dark red solid. Yield: 268 mg (42%). ^{1}H NMR (400 MHz, DMSO-d_6 with a small amount of ascorbic acid): δ 8.82 (d, J = 8.8 Hz, 2H), 8.17 (d, J = 7.9 Hz, 4H), 7.94–8.00 (m, 4H), 7.73 (d, J = 6.4 Hz, 4H). ESI-MS: *m/z* = 639.0 $[M + H]^+$ (calcd: 639.0), 661.0 $[M + Na]^+$ (calcd: 661.0).

*2.1.3. Synthesis of Ru(bda)(4-Cl-pic)$_2$ (complex **3**)*

A similar procedure for the preparation of complex **1** was adopted using 4-chloropyridine (0.5 ml) as the axial ligand. Complex **3** was obtained as a dark red solid. Yield: 228 mg (40%). ^{1}H NMR (400 MHz, DMSO-d_6): δ 8.71 (d, J = 6.7 Hz, 2H), 7.93 (m, 4H), 7.75 (d, J = 8.0 Hz, 4H), 7.47 (d, J = 8.0 Hz, 4H). ESI-MS: *m/z* = 570.9 $[M + H]^+$ (calcd: 570.9), 592.9 $[M + Na]^+$ (calcd: 592.9).

A small amount of purified powder of complex **3** was dissolved in CH_2Cl_2 and MeOH (*V*:*V* = 10:1). This solution was transferred to a tube in a Schlenk bottle. Slow diffusion of ether into the mixture at room temperature for 3 days afforded dark red crystals suitable for X-ray analysis.

*2.1.4. Synthesis of Ru(bda)(4-^{t}Bu-pic)$_2$ (complex **4**)*

A similar procedure for the preparation of complex **1** was adopted, using 4-*tert*-butylpyridine (0.5 ml) as the axial ligand. Complex **4** was obtained as a dark red solid. Yield: 251 mg (41%) ^{1}H NMR (400 MHz, DMSO-d_6): δ 8.69 (d, J = 8.0 Hz, 2H), 7.91 (d, J = 6.8 Hz, 2H), 7.84 (t, J = 7.6 Hz, 2H), 7.57 (d, J = 6.8 Hz, 4H), 7.29 (d, J = 5.4 Hz, 4H), 1.13 (s, 18H). ESI-MS: *m/z* = 615.1 $[M + H]^+$ (calcd: 615.1), 637.1 $[M + Na]^+$ (calcd: 637.1).

2.2. Characterizaion

The ^{1}H NMR data were recorded at 298 K with a 400 MHz of Bruker Avance spectrometer. Mass spectrometry (MS) measurements were performed by electrospray ionization (ESI) on an HP 1100 MSD instrument. Ultrovilot-visible (UV-Vis) absorption spectra were measured on an Agilent 8453 spectrophotometer. The electrochemical measurements were recorded with a CHI 660D electrochemical potentiostat, using a glassy carbon disk (diameter 3 mm) working electrode, polished successively with 3 and 1 mm diamond pastes and rinsed with ion-free water before use, a platinum wire as the counter electrode, and an Ag/AgCl electrode (3 mol/L KCl aqueous solution) as the reference electrode. Cyclic voltammograms (CVs) were obtained in a phosphate buffer (pH 7.0) or a CF_3SO_3H aqueous solution (pH 1.0) containing 10% MeCN.

2.3. Catalytic water oxidation

The catalytic water oxidation reactions were investigated driven by Ce^{IV} or visible light. Oxygen evolutions were monitored by GC (a GC 7890T instrument with a thermal conductivity detector, a 5 Å molecular sieve column, and using Ar as the carrying gas). When using Ce^{IV} as an oxidant in pH 1.0 solutions, the oxygen evolution was recorded with an oxygen sensor (Ocean Optics FOXY-OR125-G probe and Ocean Optics MFPF-100 fluorometer). The light-driven water oxidation reactions were illuminated with a Xe lamp (500 W) with a cut-off filter (λ > 400 nm). The gas sample was taken by syringe from the headspace of the reaction bottle and analyzed by GC.

2.3.1. Catalytic water oxidation with Ce^{IV} as oxidant

A typical reaction was performed in a 50 ml Schlenk bottle with a total volume (including the gas phase and the solution) of 82 ml. An oxygen sensor was placed in the headspace. The aqueous CF_3SO_3H solution (initial pH = 1.0; 3 ml) containing 1.5 g of Ce^{IV} was added to the flask and degassed with Ar for 20 min. A degassed acetonitrile/water (1/1, *V*/*V*) solution of the catalyst (100 μl, 1.5 mmol/L) was injected into the solution. The generated O_2 was then measured and recorded vs time.

2.3.2. Photocatalytic water oxidation

In a typical experiment, $Ru(bpy)_3Cl_2$ (3.2 mg, 5 μmol) and $Na_2S_2O_8$ (12 mg, 50 μmol) in a phosphate buffer (pH 7.0, 5 ml) containing 10% acetonitrile and Ru catalyst (50 μl, 1 mmol/L) were added to a Schlenk bottle (total volume of 82 ml). The solution was degassed with N_2 for 20 min prior to irradiation. The light-driven water oxidation reaction was started by irradiation at 20 °C (in a circulated water cooling bath) using an Xe lamp (500 W) with a cut-off filter (λ > 400 nm). The generated O_2 was then measured by GC.

3. Results and discussion

3.1. Characterization of the Ru complexes

In this study, a two-step synthetic procedure was successfully developed to prepare the Ru complexes **1**–**4**. The overall yields are superior to the previous one-pot reaction method [26]. This provides an easy and convenient way to prepare similar Ru complexes bearing bipyridine dicarboxylate as the equatorial ligand backbone and pyridine derivatives as axial ligands. Because Ru(II) compounds are easily oxidized to Ru(III) in the presence of molecular oxygen, a small amount of ascorbic acid was added as a reducing agent to some NMR samples to obtain well-defined signals in ^{1}H NMR spectra. The proton signals of the substituted pyridines were generally shifted to low field by coordination to the Ru center in ^{1}H NMR spectra.

*3.1.1. X-ray crystal structure of complex **3***

The single-crystal X-ray diffraction (XRD) data were collected on a Bruker Smart Apex II CCD diffractometer with graphite-monochromated Mo-K_α radiation (λ = 0.071073 nm) at 298 K using the omega scans. SAINT was used for data processing. Intensity data were corrected for absorption using SADABS. All structures were solved by direct methods and refined on F^2 against full-matrix least-squares methods by using the SHELXTL 97 program package. All non-hydrogen atoms

Table 1
Selected bond lengths and bond angles for complex **3**.

Bond length (Å)	Bond angle (°)
Ru(1)–N(1) 2.070(8)	N(1)–Ru(1)–N(2) 173.6(3)
Ru(1)–N(2) 2.074(8)	N(1)–Ru(1)–O(2) 89.6(3)
Ru(1)–N(3) 1.910(8)	N(2)–Ru(1)–O(3) 89.9(3)
Ru(1)–N(4) 1.925(7)	O(2)–Ru(1)–O(3) 122.2(2)
Ru(1)–O(2) 2.182(7)	N(4)–Ru(1)–N(1) 90.9(3)
Ru(1)–O(3) 2.166(7)	N(4)–Ru(1)–N(2) 93.7(3)
O(3)–C(12) 1.282(11)	N(4)–Ru(1)–O(2) 160.0(3)
O(4)–C(12) 1.237(11)	N(4)–Ru(1)–O(3) 77.8(3)
O(1)–C(1) 1.237(10)	N(3)–Ru(1)–N(1) 93.7(3)
O(2)–C(1) 1.300(11)	N(3)–Ru(1)–N(2) 91.2(3)
C(1)–C(2) 1.500(12)	N(3)–Ru(1)–O(2) 77.4(3)
C(11)–C(12) 1.522(14)	N(3)–Ru(1)–O(3) 160.4(3)

were refined anisotropically. Hydrogen atoms were located by geometrical calculation. Details of crystal data, data collections, and structure refinements are summarized in Table 1. These data can be obtained free of charge from the Cambridge Crystallographic Data Centre via www.ccdc.cam.ac.uk/data_request/cif. CCDC number: 926182.

The X-ray crystal structure of complex **3** (Fig. 1) reveals a distorted octahedron configuration around the ruthenium center, which agrees with the structure derived from the ^{1}H NMR spectrum. The average Ru–N distance was 1.995 Å, while the average distance of the Ru–O bonds is 2.174 Å. The O_2–Ru–O_3 angle of 122.2° is much larger than that of an ideal octahedron and this wide angle was also seen in complex **A** [26]. This wide angle could facilitate the coordination of water as the seventh ligand, which is thought to be the initial step in the oxidation reaction, followed by a series of PCET (proton coupled electron transfer) processes [26].

3.1.2. Electrochemistry

Complexes **1** and **3** are soluble in organic solvents such as

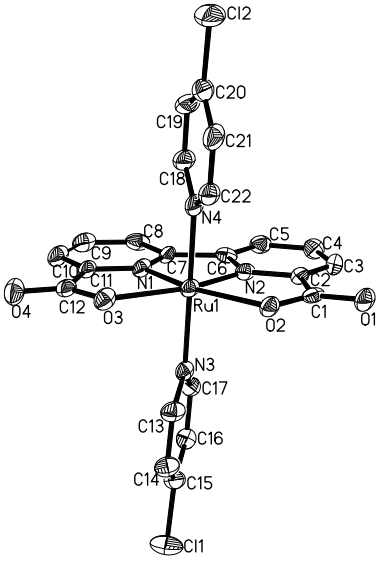

Fig. 1. Crystal structure of complex **3.** The hydrogen atoms were omitted for clarity.

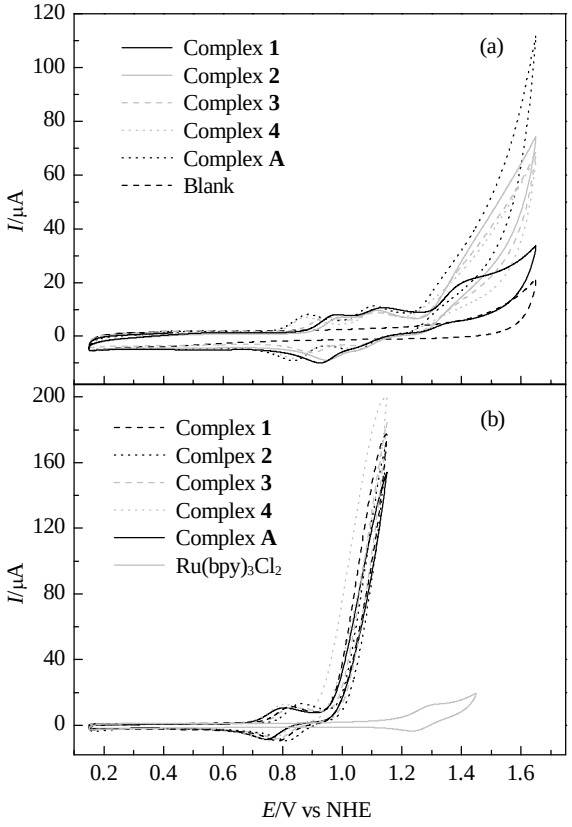

Fig. 2. (a) CVs of complexes **1**–**4** and **A** (1 mmol/L) in CF_3SO_3H aqueous solutions (pH 1.0) containing 10% MeCN and a blank for comparison; (b) CVs of complexes **1**–**4** and **A** (1 mmol/L) in a phosphate buffer (pH 7.0) containing 10% MeCN as well as $[Ru(bpy)_3]Cl_2$ (1 mmol/L) under the same conditions.

MeOH and MeCN but only sparingly soluble in water. To aid comparison, the spectroscopic and catalytic property studies of **1**–**4** were carried out in aqueous solutions containing 10% MeCN. CVs of complexes **1**–**4** at pH 1.0 and pH 7.0 are shown in Fig. 2, and the related electrochemical data are listed in Table 2.

Generally, in pH 1.0 the CVs show two reversible redox couples around 0.9 and 1.1 V (Table 2) attributed to the two single electron processes of $Ru^{II/III}$ and $Ru^{III/IV}$. The onset potential of water oxidation for these compounds occurs around 1.3 V, which is comparable to $Ru^{II}(bda)(pic)_2$, demonstrating a low overpotential for water oxidation.

The CVs of these complexes were also measured under neutral conditions in phosphate buffer solutions (pH 7.0) containing 10% MeCN. As shown in Fig. 2, the corresponding redox waves of $Ru^{II/III}$ are observed at about 0.8 V, followed by the

Table 2
Redox potentials of complexes **1**–**4** and **A** in pH 1.0 and pH 7.0 aqueous solutions respectively.

Complex	*E* (V vs NHE[a], pH 1.0)			*E* (V vs NHE[a], pH 7.0)	
	$E_{1/2}^{ox}$ ($Ru^{II/III}$)	$E_{1/2}^{ox}$ ($Ru^{III/IV}$)	E_{onset}	$E_{1/2}^{ox}$ ($Ru^{II/III}$)	E_{onset}
1	0.96	1.10	1.32	0.66	0.98
2	0.98	1.09	1.30	0.69	1.01
3	0.93	1.08	1.29	0.66	0.99
4	0.86	1.08	1.25	0.63	0.94
A	0.87	1.10	1.27	0.62	0.97

[a]$Ru(bpy)_3^{2+}$ was used as a reference with $E_{1/2}$ = 1.26 V vs NHE.

onset of the water oxidation past 0.9 V. In contrast to the electrochemical behavior under acidic conditions, the $Ru^{III/IV}$ process under neutral conditions cannot be detected by cyclic voltammetry. A similar phenomenon was also reported by other water oxidation systems with other Ru catalysts [34]. It appears that the $Ru^{III/IV}$ process is hidden by the intense water oxidation process.

Because the water oxidation potentials of complexes **1**–**4** decrease in less acidic environments, it implies that photocatalytic water oxidation could be achieved using a photosensitizer as a mediator. For example, $[Ru(bpy)_3]^{2+}$ exhibits a $Ru^{II/III}$ redox couple at 1.26 V under the identical conditions, which is higher than the onset water oxidation peaks of **1**–**4** by about 300 mV, indicating that water oxidation driven by $[Ru(bpy)_3]^{2+}$ in the presence of **1**–**4** is thermodynamically favored.

Furthermore, as shown in Fig. 2 and Table 2, the onset potentials of complex **1**–**4** in either pH 1.0 or pH 7.0 increases with the electron-withdrawing ability of the substituent groups on the *para* position of axial pyridine ligands. At pH 1.0, complex **1** exhibits the highest onset potential, where the axial 4,4′-bipyridine ligand may be protonated under acidic condition and therefore exhibits a stronger electron-withdrawing effect than the neutral groups.

3.1.3. UV-Vis spectra

The UV-Vis spectrometry of complexes **1**–**4** (5×10^{-5} mol/L) was conducted in phosphate buffer solutions (pH 7.0) containing 5% MeCN at room temperature (Fig. 3). The UV-Vis absorbance curves of the four Ru-based catalysts generally display intense absorptions from 200 to 300 nm, which are assigned to the π-π* transitions of the ligands. The weaker bands in the visible region are attributed to metal-to-ligand charge-transfer (MLCT) [35] transitions from the *d*-orbital of the metal to the π*-orbital of the ligands. It can be seen in Fig. 3 that the electron-withdrawing effect of the substituted groups on the *para* position of axial pyridine ligands is related to the energy and intensity of these bands. When the *para* substituents are varied from CF_3, Cl, and CH_3 to ^{t}Bu, the σ-donating ability of the pyridine increases accordingly and causes a red shift in the MLCT bands.

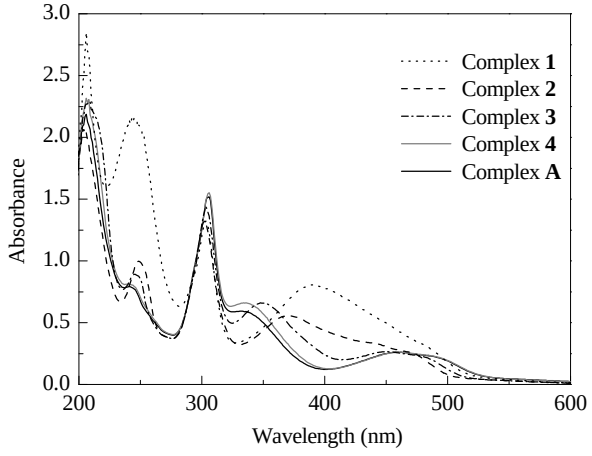

Fig. 3. UV-Vis absorbance spectra of complexes **1**–**4** and **A** (5×10^{-5} mol/L) in a phosphate buffer (pH 7.0) containing 5% MeCN.

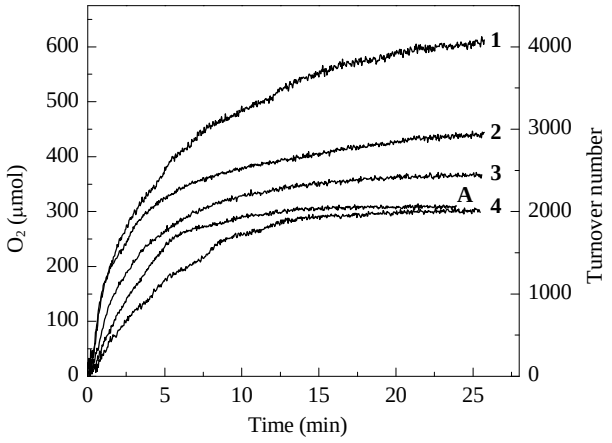

Fig. 4. Oxygen evolution curves of complexes **1**–**4** and **A** in an aqueous solution of CF_3SO_3H (initial pH 1.0, 3 ml) containing Ce^{IV} (1.5 g, 0.9 mol/L) and the catalyst (5×10^{-5} mol/L) recorded with an oxygen sensor and calibrated by GC.

3.2. Catalytic water oxidation

3.2.1. Catalytic water oxidation with Ce^{IV} as oxidant

As shown in Fig. 4 and Table 3, all four complexes exhibit high catalytic activities towards Ce^{IV}-driven water oxidation with TONs from 2000 to 4000 and TOFs from 6.0 to 11.2 s^{-1}.

The TONs and TOFs of these Ru complexes were found to depend on the electron-withdrawing effect of the substituted groups on the *para* position of the axial pyridine ligands. Complex with more electron-withdrawing group exhibited more activity towards water oxidation, for example, **2** ($-CF_3$) > **3** ($-Cl$) > **A** ($-CH_3$) > **4** ($-^t$Bu) (Table 3). The highest TON of 4319 was obtained using complex **1** due to the protonation of the axial 4,4′-bipyridine ligand under acidic conditions.

3.2.2. Photocatalytic water oxidation

As shown in Fig. 5 and Table 3, all four complexes exhibit high photocatalytic activities with $Ru(bpy)_3Cl_2$ as a photosensitizer and $Na_2S_2O_8$ as a sacrificial electron acceptor in a three-component system. Complex **1** was not the most active catalyst of the four complexes in contrast to the Ce(IV)-driven water oxidation. This may be due to the axial ligands not being protonated under the neutral conditions (pH 7.0). The most active catalyst was complex **2** with 4-(trifluoromethyl)pyridine as the most electron-withdrawing group of the axial ligands, which gave a TON of 275. Again this implies that the TON increases with the increasing electron withdrawing ability of the axial ligands in this series of Ru complexes. Because the se-

Table 3
TONs and TOFs of complexes **1–4** and **A** in the chemical water oxidation with Ce^{IV} as oxidant and visible-light-driven water oxidation.

Complex	Chemical water oxidation		TON for light-driven water oxidation
	TON	TOF[a] (s^{-1})	
1	4319	11.2	125
2	3397	10.1	275
3	2492	7.7	200
4	2034	4.5	78
A	2070	6.0	97

[a] Calculated within the initial 3 min of oxidation.

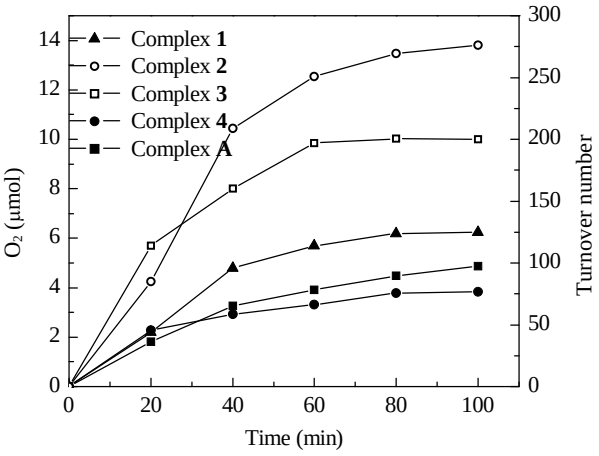

Fig. 5. Visible-light-driven oxygen evolution catalyzed by complexes **1**–**4** and **A** (1×10^{-5} mol/L) in 5 ml of a phosphate buffer solution (pH 7.0) containing $Ru(bpy)_3Cl_2$ (1×10^{-3} mol/L) and $Na_2S_2O_8$ (1×10^{-2} mol/L).

quence of the electron-withdrawing ability of the substituted groups on the *para* position of axial pyridine ligands is **2** ($-CF_3$) > **3** (–Cl) > **1** (–Py) > **A** ($-CH_3$) > **4** ($-^t$Bu) under neutral conditions, this matches the sequence of activities of these Ru complexes towards light-driven water oxidation (Table 3).

4. Conclusions

Through a two-step synthetic method a family of robust Ru^{II}-based water oxidation catalysts involving the negatively charged equatorial ligand 2,2′-bipyridine-6,6′-dicarboxylate and *para*-substituted pyridines has been prepared and characterized. Their catalytic abilities in the water oxidation with Ce^{IV} as oxidant or driven by visible light were investigated under acid and neutral conditions, respectively. It was found that axial ligands with electron-withdrawing substituent improves the activity of the catalyst towards water oxidation. These results show the effect of the organic ligands on water oxidation, and supplement our previous studies on the variations of the axial ligand. This will provide basic principles for the design of more efficient WOCs. Moreover, the low catalytic overpotentials of these catalysts are favorable for visible-light-driven water oxidation, indicating their possible application in photovoltaic devices for the overall splitting of water.

References

[1] Lewis N S, Nocera D G. *Proc Natl Acad Sci USA*, 2006, 103: 15729
[2] Barber J. *Chem Soc Rev*, 2009, 38: 185
[3] Dau H, Zaharieva I. *Acc Chem Res*, 2009, 42: 1861
[4] Yagi M, Narita K. *J Am Chem Soc*, 2004, 126: 8084
[5] Gao Y, Akermark T, Liu J H, Sun L C, Akermark B. *J Am Chem Soc*, 2009, 131: 8726
[6] Hull J F, Balcells D, Blakemore J D, Incarvito C D, Eisenstein O, Brudvig G W, Crabtree R H. *J Am Chem Soc*, 2009, 131: 8730
[7] Savini A, Bellachioma G, Ciancaleoni G, Zuccaccia C, Zuccaccia D, Macchioni A. *Chem Commun*, 2010, 46: 9218
[8] Lalrempuia R, McDaniel N D, Muller-Bunz H, Bernhard S, Albrecht M. *Angew Chem, Int Ed*, 2010, 49: 9765
[9] Hetterscheid D G H, Reek J N H. *Chem Commun*, 2011, 47: 2712
[10] Savini A, Bellachioma G, Bolano S, Rocchigiani L, Zuccaccia C, Zuccaccia D, Macchioni A. *ChemSusChem,* 2012, 5: 1415
[11] McCool N S, Robinson D M, Sheats J E, Dismukes G C. *J Am Chem Soc*, 2011, 133: 11446
[12] Wasylenko D J, Ganesamoorthy C, Borau-Garcia J, Berlinguette C P. *Chem Commun*, 2011, 47: 4249
[13] Dogutan D K, McGuire R Jr, Nocera D G. *J Am Chem Soc*, 2011, 133: 9178
[14] Leung C F, Ng S M, Ko C C, Man W L, Wu J S, Chen L J, Lau T C. *Energy Environ Sci*, 2012, 5: 7903
[15] Ellis W C, McDaniel N D, Bernhard S, Collins T J. *J Am Chem Soc*, 2010, 132, 10990
[16] Fillol J L, Codolà Z, Garcia-Bosch I, Gómez L, Pla J J, Costas M. *Nat Chem*, 2011, 3: 807
[17] Sala X, Romero I, Rodriguez M, Escriche L, Llobet A. *Angew Chem, Int Ed,* 2009, 48: 2842
[18] Gersten S W, Samuels G J, Meyer T J. *J Am Chem Soc*, 1982, 104: 4029
[19] Wada T, Tsuge K, Tanaka K. *Angew Chem*, *Int Ed*, 2000, 39: 1479
[20] Sens C, Romero I, Rodriguez M, Llobet A, Parella T, Benet-Buchholz J. *J Am Chem Soc*, 2004, 126: 7798
[21] Zong R F, Thummel R P. *J Am Chem Soc*, 2005, 127: 12802
[22] Xu Y H, Fischer A, Duan L L, Tong L P, Gabrielsson E, Akermark B, Sun L C. *Angew Chem*, *Int Ed*, 2010, 49: 8934
[23] Jiang Y, Li F, Zhang B B, Li X N, Wang X H, Huang F, Sun L C. *Angew Chem*, *Int Ed*, 2013, 52: 3398
[24] Yang X F, Baik M H. *J Am Chem Soc*, 2004, 126: 13222

Graphical Abstract

Chin. J. Catal., 2013, 34: 1489–1495 doi: 10.1016/S1872-2067(12)60600-7

Chemical and photocatalytic water oxidation by mononuclear Ru catalysts

Yi Jiang, Fei Li*, Fang Huang, Biaobiao Zhang, Licheng Sun*
Dalian University of Technology, China;
KTH Royal Institute of Technology, Sweden

Mononuclear ruthenium complexes based on the bipyridine-dicarboxylate (bda) ligand were prepared and showed high catalytic efficiencies for chemical and photochemical water oxidation, a key challenge for solar energy conversion into fuels. The more electron-withdrawing substituents on the axial ligands of the catalysts lead to higher activities towards water oxidation.

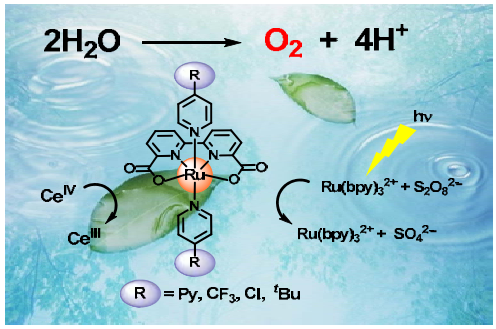

[25] Concepcion J J, Jurss J W, Norris M R, Chen Z F, Templeton J L, Meyer T J. *Inorg Chem*, 2010, 49: 1277
[26] Duan L L, Fischer A, Xu Y H, Sun L C. *J Am Chem Soc*, 2009, 131: 10397
[27] Duan L L, Xu Y H, Zhang P, Wang M, Sun L C. *Inorg Chem*, 2010, 49: 209
[28] Nyhlen J, Duan L L, Aakermark B, Sun L C, Privalov T. *Angew Chem, Int Ed*, 2010, 49: 1773
[29] Duan L L, Bozoglian F, Mandal S, Stewart B, Privalov T, Llobet A, Sun L C. *Nat Chem*, 2012, 4: 418
[30] Duan L L, Araujo C M, Ahlquist M S G, Sun L C. *Proc Natl Acad Sci USA*, 2012, 109: 15584
[31] Wang L, Duan L L, Stewart B, Pu M P, Liu J H, Privalov T, Sun L C. *J Am Chem Soc*, 2012, 134: 18868
[32] Li F, Jiang Y, Zhang B B, Huang F, Gao Y, Sun L C. *Angew Chem, Int Ed*, 2012, 51: 2417
[33] Duliere E, Devillers M, Marchand-Brynaert J. *Organometallics*, 2003, 22: 804
[34] Concepcion J J, Tsai M K, Muckerman J T, Meyer T J. *J Am Chem Soc*, 2010, 132: 1545
[35] Gilbert J A, Eggleston D S, Murphy Jr. W R, Geselowitz D A, Gersten S W, Hodgson D J, Meyer T J. *J Am Chem Soc*, 1985, 107: 3855

单核钌催化剂化学催化和光催化水氧化反应

姜 毅[a], 李 斐[a,*], 黄 芳[a], 张彪彪[a], 孙立成[a,b,#]
[a]大连理工大学环境与生命科学学院, 精细化工国家重点实验室, 辽宁大连116024
[b]瑞典皇家工学院化学科学与工程学院化学系, 瑞典斯德哥尔摩10044

摘要: 合成了一系列含有不同对位取代基团的吡啶轴向配体的单核钌化合物Ru(bda)(pic)$_2$ (H_2bda = 2,2'-联吡啶-6,6'-二羧酸; pic = 对甲基吡啶), 对化合物的结构进行了核磁、质谱和X射线单晶衍射表征, 并在中性和酸性条件下研究了这些化合物的电化学性质. 以硝酸铈铵为氧化剂, 对催化剂的催化活性进行了测试, 并以$[Ru(bpy)_3]^{2+}$为光敏剂, $S_2O_8^{2-}$为电子牺牲剂, 在三组分体系中考察了这些化合物的光催化活性. 研究发现, 在化学法水氧化反应中, 化合物**1**由于其轴向配体4,4'-联吡啶在酸性条件下能够发生质子化, 从而增强了吸电子效应, 因此表现出最高的催化活性, 催化循环数达到4000. 在光催化水氧化反应中, 化合物**2**因其轴向配体具有最强的吸电子能力而表现出最高的催化活性, 反应2 h的催化循环数达到270. 结果表明, 轴向配体的吸电子能力明显提高了这类Ru催化剂催化水氧化反应活性.

关键词: 分解水; 水氧化; 钌配合物; 吸电子效应; 光催化

收稿日期: 2013-03-22. 接受日期: 2013-04-10. 出版日期: 2013-08-20.
*通讯联系人. 电话: (0411)84986247; 传真: (0411)84986245; 电子信箱: lifei@dlut.edu.cn
#通讯联系人. 电话/传真: (+46)-8-7912333; 电子信箱: lichengs@kth.se
基金来源: 国家自然科学基金(21106015, 21120102036, 20923006); 国家重点基础研究发展计划(973计划, 2009CB220009); 高等学校博士学科点专项科研基金(20110041120005); 瑞典能源部K&A Wallenberg基金.
本文的英文电子版由Elsevier出版社在ScienceDirect上出版(http://www.sciencedirect.com/science/journal/18722067).